The Astrophysical Journal, 689:219–224, 2008 December 10

THE TRUE SHAPES OF THE DUMBBELL AND THE RING

Sun Kwok and Sze-Ning Chong
Department of Physics, University of Hong Kong, Pokfulam Road, Hong Kong, China; sunkwok@hku.hk

Nico Koning
Department of Physics and Astronomy, University of Calgary, Calgary, AB T2N 1N4, Canada

Trung Hua
Laboratorie d'Astrophysique de Marseille, Marseille, France

and

Chi-Hung Yan
Institute of Astronomy and Astrophysics, Academia Sinica, Taipei, Taiwan
Received 2008 May 10; accepted 2008 July 24

ABSTRACT

Using images centered around the 2.12 μm line of molecular hydrogen obtained with the Wide Field Infrared Camera on the Canada-France-Hawaii Telescope, we show that in spite of the different apparent morphologies, the Dumbbell Nebula and the Ring Nebula share the same intrinsic three-dimensional triple biconic structure.

Subject headings: infrared: ISM — planetary nebulae: general — planetary nebulae: individual (NGC 6720, NGC 6853)

1. INTRODUCTION

Our modern understanding of planetary nebulae is that their morphology is shaped by dynamical interactions between successive stellar winds (Balick 1987; Kwok 2000). While the winds from the planetary nebula progenitor asymptotic giant branch (AGB) star are likely to be spherically symmetric, there is strong evidence that the fast winds that develop during the post-AGB phase are nonisotropic, or even highly collimated. The often-observed bipolar morphology in planetary nebulae (e.g., NGC 2346, NGC 6302) is believed to be due to collimated fast winds carving out a cavity from the remnants of the spherical AGB winds. Tying the diverse range of observed morphologies of planetary nebulae to the dynamical models represents one of the major challenges of planetary nebula research today.

The Dumbbell Nebula (NGC 6853, M27) and the Ring Nebula (NGC 6720 and M57) are among the four planetary nebulae included in the Messier Catalogue in 1784. As their names imply, they have apparent shapes of a dumbbell and a ring, respectively. This classification has not substantially changed after their initial discovery over 200 years ago. The difficulty in comparing predictions from theoretical dynamical models with observations is that often we do not know the true intrinsic three-dimensional (3D) structure of planetary nebulae, even well-observed nebulae such as NGC 6853 and NGC 6720. For example, the structure of NGC 6720 has been proposed to be a torus (Minkowski & Osterbrock 1960), a flat ring (Hua & Louise 1970), a cylinder (Proisy 1974; Goad 1975), a spheroid (Kupferman 1983), a bipolar (Bryce et al. 1994), or an ellipsoid (Guerrero et al. 1997). Modern CCD observations of NGC 6853 have found that the "dumbbell" is surrounded by an elliptical nebula of $8' \times 5'$, with a faint halo outside (Balick et al. 1992; Hua et al. 1998; Meaburn et al. 2005). Similarly, the main "ring" of NGC 6720 is surrounded by a double outer halo (Balick et al. 1992). The relationship between the main part of the nebula (the ring) and the fainter double outer halos has never been adequately explained. The situation for NGC 6853 is not much better (Meaburn et al. 2005).

The 2.12 μm $v = 1\text{–}0\ S(1)$ line of molecular hydrogen has been widely used as a tracer of shock excitation. Advances in near-infrared imaging has made it possible to use H_2 images to outline the regions of wind interactions in planetary nebulae (Zuckerman & Gatley 1988; Kastner et al. 1996). As a result, H_2 images may be our most direct link to the dynamical processes involved. This is in contrast to the use of atomic emission lines, whose brightness distribution are affected by ionization and excitation conditions.

2. OBSERVATIONS AND RESULTS

Observations were obtained using the Wide-field Infrared Camera (WIRCam) on the Canada-France-Hawaii Telescope (CFHT) under the program 06AT03 on 2006 April 16. WIRCam consists of four HAWAII2-RG detectors, each having a 2048×2048 pixel format with a pixel scale of $0.3''$. The total field of view of the camera is $20' \times 20'$. The images of NGC 6853 were taken with a narrowband molecular hydrogen filter (central wavelength 2.122 μm, bandwidth 0.032 μm) and the broad band K_s filter (central wavelength 2.146 μm, bandwidth 0.325 μm). Observations of NGC 6853 at the CFHT were made in the nodding mode, where a five-position dither pattern is made on target, and then an off-target (sky) frame is taken. The exposure time on each frame for each filter is 30 s and 6 s, respectively. Observations of the standard stars FS30, FS140, FS146, FS148, and FS152 were made with the K_s filter, for an exposure time of 10 s. Standard bias subtraction, flat-fielding, and bad pixel masking were performed. The sky background of each image was subtracted based on the comoving-averaged frame, which is made using the images taken during a certain period of observations. Cross-talk was also removed after sky background subtraction. Images were stacked together to improve the dynamic range and to remove defects. Astrometry and photometry corrections were performed against the 2MASS catalog in order to correct the image distortion and flux level. Since the stacked H_2 and K_s images have different sizes, excess pixels were cut by the IRAF utility IMCOPY to trim the H_2 and K_s images to the same size. The IRAF utility IMSHIFT

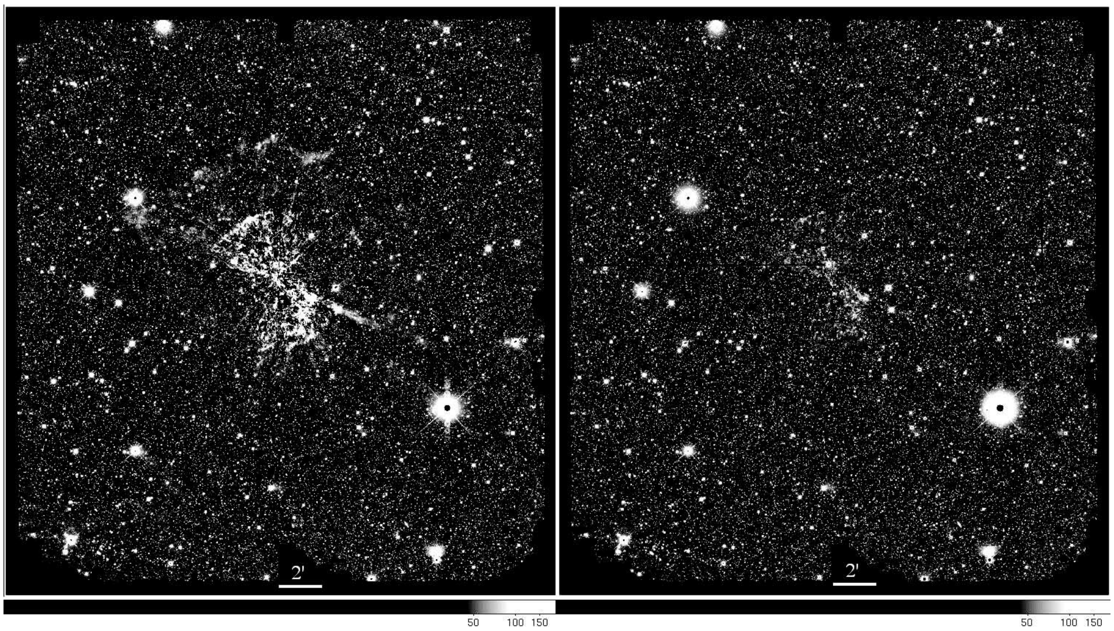

FIG. 1.—CFHT WIRCam H_2 image (*left*) and K_s image (*right*) of NGC 6853. North is up and east is to the left.

was used to shift the images in order to match the background stars.

The H_2 and K_s images of NGC 6853 are shown in Figure 1. A difference image of $H_2 - K_s$ is shown in Figure 2. A pair of bright fan-shape nebulosities with sharp outer boundaries can clearly be seen. Beyond this pair, two more pairs of fainter outer fans are also visible. If we approximate the outer boundary arcs by three circles centered on the central star, they have radii of 190^{+4}_{-6}, 277^{+18}_{-11}, and 371^{+14}_{-10} arcsec, respectively. The sides of the three fans can be defined by a pair of straight lines oriented at position angle (P.A., measured from north to east) of 0° and 64°, suggesting that the symmetry axis lies at a P.A. of 32°. The narrowness of the base of the fans suggests that the bipolar outflows are confined by a high-density, unseen equatorial region.

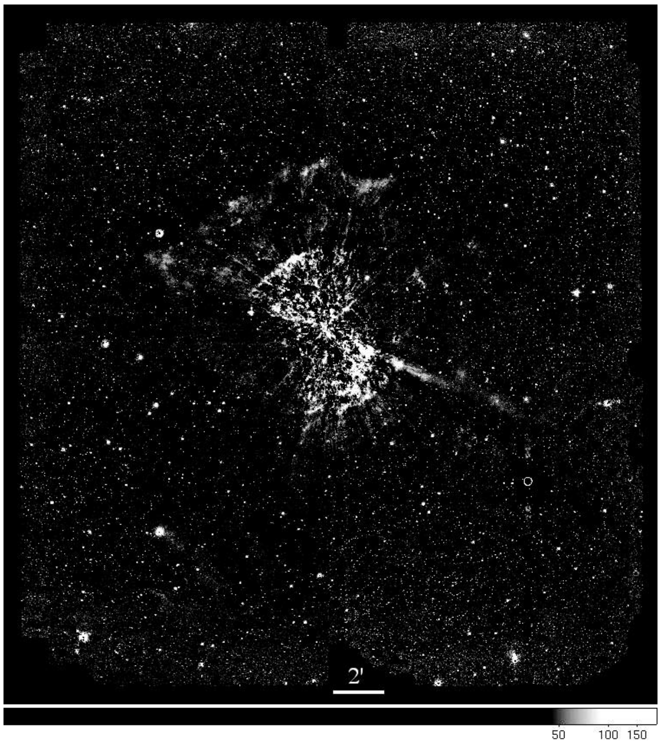

FIG. 2.—$H_2 - K_s$ difference image of NGC 6853.

These three pairs of bipolar nebulae have a common center located at R.A. (2000) = $19^{\mathrm{h}}59^{\mathrm{m}}36.340^{\mathrm{s}}$, decl. (2000) = +22°43′16.09″. A series of radial streamers can be seen emanating

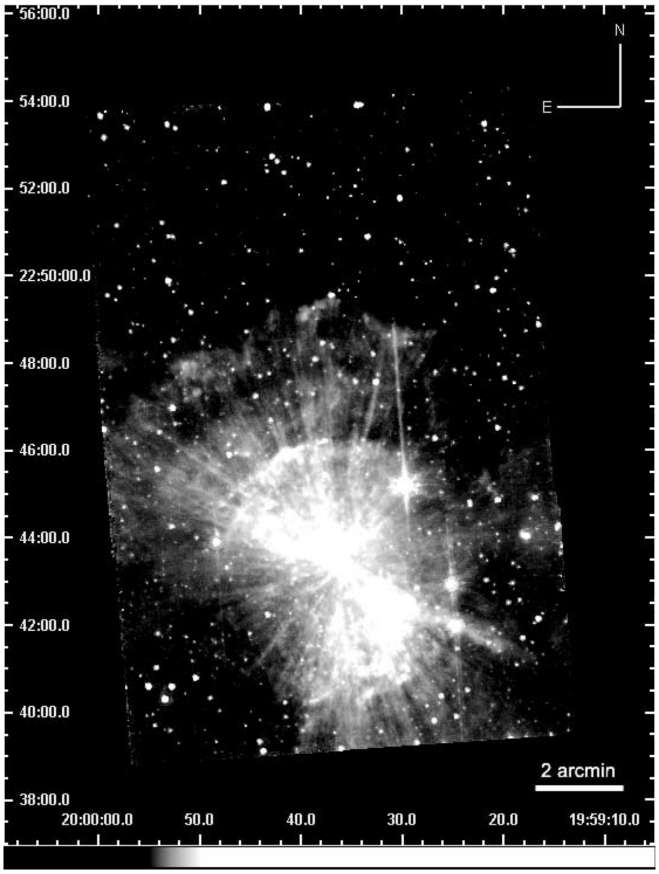

FIG. 3.—IRAC 8 μm image of NGC 6853, observed as part of the *Spitzer Space Telescope* GTO program.

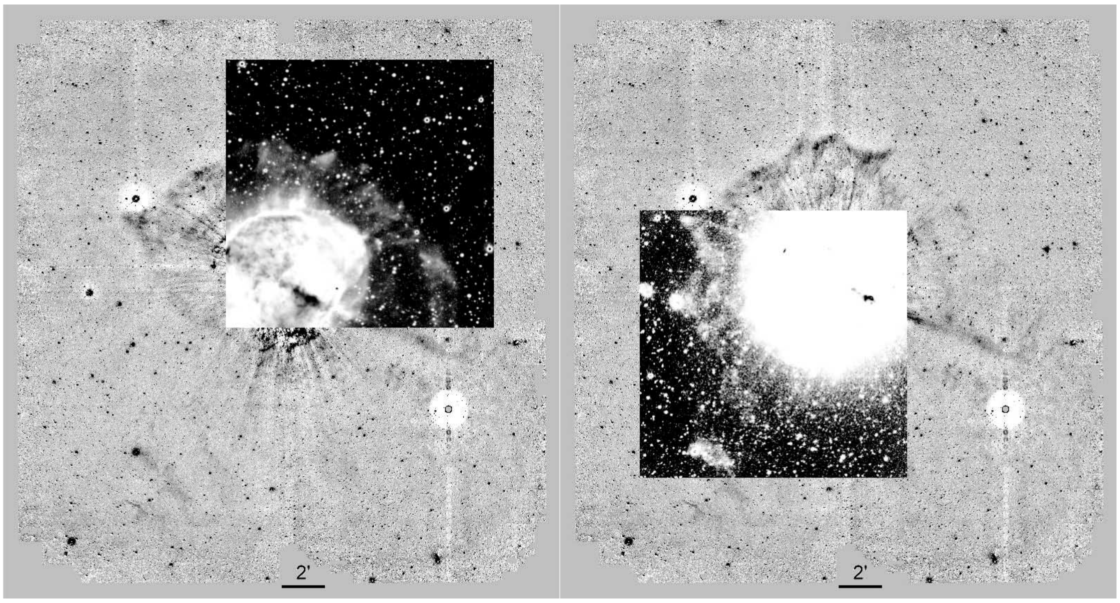

FIG. 4.—[N II] image (*inset*) superimposed on the H_2-K_s image of NGC 6853. The main nebula is overexposed intentionally in order to show the fainter outer structures. The NW corner of the nebula is shown in the left image, and the SE corner is shown in the right image.

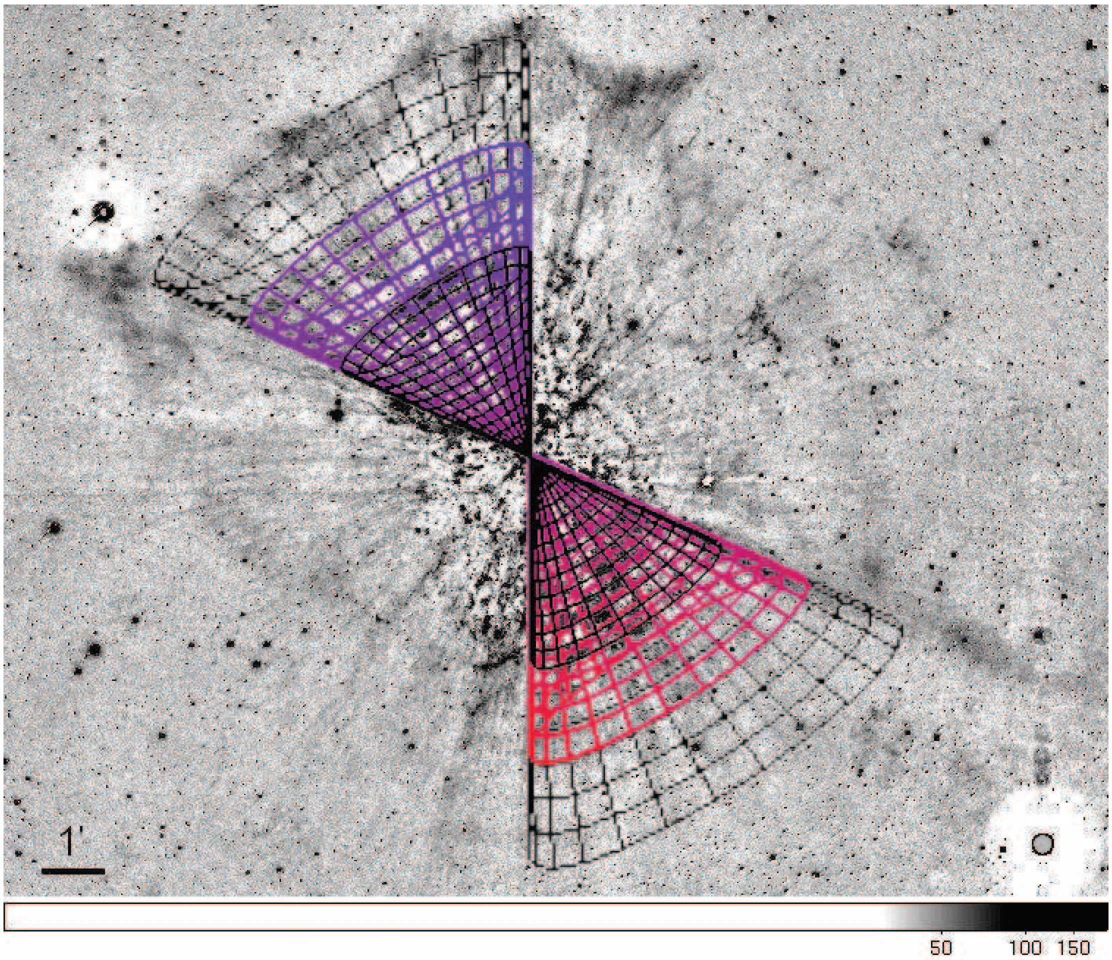

FIG. 5.—Schematic drawing of triple conic sections as approximations to the triple bipolar lobes of NGC 6853. The outer edges of the lobes are approximated by the rims of the open cones on the plane of the sky. From the ellipticity of the rim, we deduce that the bipolar axis lies at an angle of 15° from the plane of the sky.

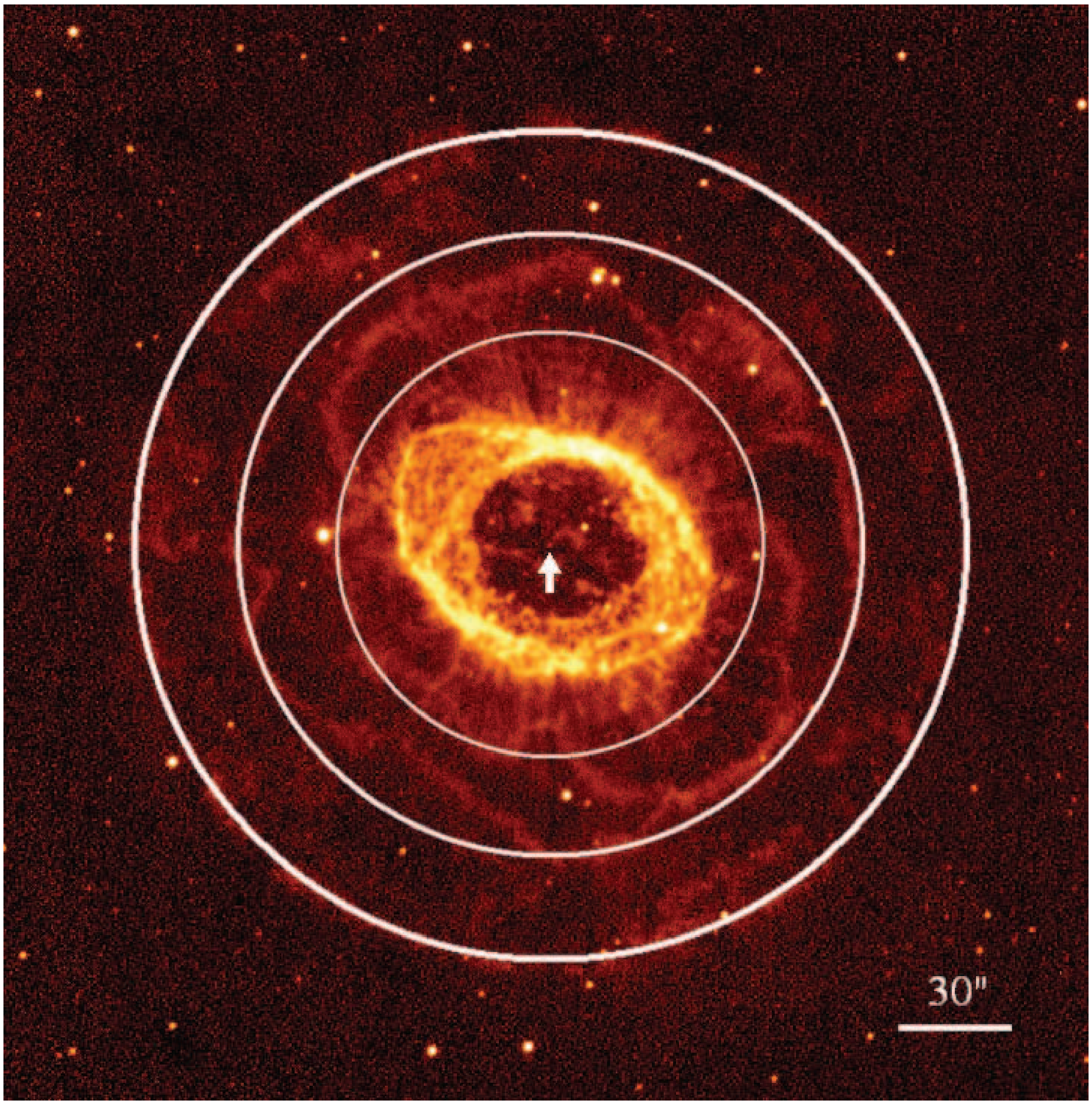

Fig. 6.—Conic sections of Fig. 5 rotated to an orientation of 90°, scaled by (890 pc/420 pc) = 2.12, and superimposed on the H_2 image of NGC 6720 taken by David Thompson at Calar Alto Observatory. This scaling factor of 2.12 could reflect a combination of the relative distances of the two objects, as well as a difference in outflow velocities of the cones in the two objects. The white arrow indicates the center of the set of cones, which is also the position of the central star, at R.A. (2000) = $18^{h}53^{m}35.079^{s}$, decl. (2000) = $+33°01'45.03''$.

from the central star in all directions, more prominently in the polar (NE-SW) directions, but also in the equatorial regions. These radial features are visible in a previous H_2 image of NGC 6853 by Kastner et al. (1996), but are shown in greater detail here. The presence of such radial streams is confirmed by the 8 μm Infrared Array Camera (IRAC) image of NGC 6853 taken from the *Spitzer Space Telescope* (Fig. 3; see also Hora 2006). Almost one-to-one correspondence of the radial rays can be found between the H_2 and 8 μm images, suggesting that they share the same origin.

Figure 4 shows a superposition of the H_2-K_s image with the optical [N II] image of the nebula. The optical image was obtained with the Observatoire de Haute-Provence (OHP) 1.2 m telescope on 1997 September 5. Images were taken with the Tektronix Tk1024 camera with 24 μm pixel size, providing a resolution of 0.686″ per pixel. The [N II] filter has a central wavelength of 6583 Å and a width of 10 Å. An outer halo can clearly be seen in the [N II] image, and the outer boundary of the halo matches well with the extent of the outer fan of the H_2-K_s image. While both [N II] and H_2 halos cover most angles, along the equatorial direction the former is more obvious and extends farther out than the latter. It is possible that the outer halo as seen in [N II] is spherical but the segment in the polar directions is better illuminated in H_2 due to shock excitation by a collimated fast wind.

3. DISCUSSION

The existence of pairs of inner and outer fans suggests that they represent projections of 3D conic sections on the sky. Figure 5 shows a schematic drawing of this 3D structure. By fitting the projected openings of the cones with the observed curvature of the arcs, we were able to derive the 3D orientation of the cones in the sky. We assume that the cones have circular openings, and derive their orientation angle by measuring the ellipticity of the projected openings of the cones in the sky. The opening angles of the cones were derived by visually matching the projected edges of the cones to the observed straight edges of the fans. The cones shown in Figure 5 have a common axis oriented at an angle of 15° ± 5° from the plane of the sky, a common opening angle

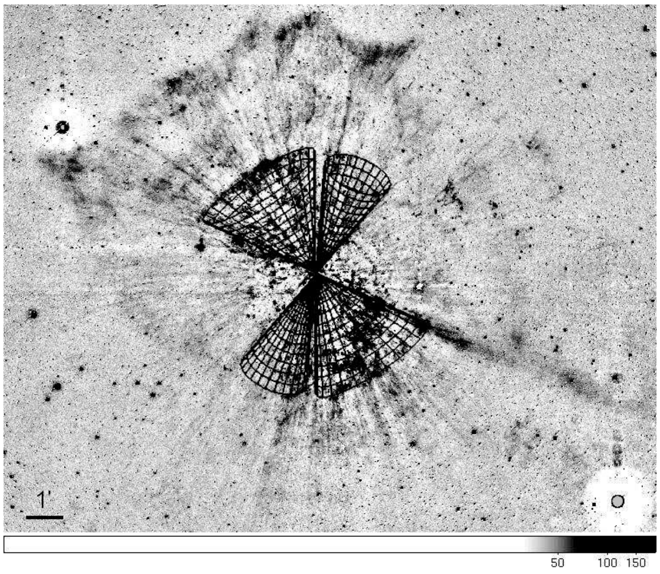

Fig. 7.—Schematic drawing of the two possible bipolar axes of the Dumbbell Nebula.

of 0.30 ± 0.04π, and radii of 212^{+6}_{-4}, 311^{+13}_{-5}, and 413^{+13}_{-9} arcsec, respectively.

It occurs to us that if this 3D structure is rotated to an orientation with the axis nearly perpendicular to the sky, the projections of the two outer cones would resemble the two outer halos of NGC 6720. Figure 6 shows a schematic of the cones of NGC 6853 rotated to the pole-on orientation, with the dimensions scaled from a distance of 420 pc (for NGC 6853; Benedict et al. 2003) to an assumed distance of 890 pc for NGC 6720. Comparison of this image to the observed H_2 image of NGC 6720 suggests strongly that NGC 6853 and NGC 6720 have the same intrinsic 3D structure. The main difference between NGC 6720 and NGC 6853 is that NGC 6720 has a bright central torus. If such a torus (or a density-enhanced equatorial ring) is also present in NGC 6853, it would be nearly edge-on.

The existence of three pairs of cones with similar opening angles in NGC 6853 suggests that they were created by interactions between a single fast outflow with three separate shells in the AGB envelope. Assuming a distance of 420 pc (Benedict et al. 2003) and that the fast outflow has an expansion velocity of V, the dynamical ages of the three cones are $t = 420$, 620, and $820 \times (V/10\ \mathrm{km\ s^{-1}})^{-1}$ yr, respectively. The possibility that AGB mass loss may have multiple discrete structures has been known for some time, from the observation of concentric circular arcs seen in scattered light in AGB stars (Mauron & Huggins 1999) and protoplanetary nebulae (Kwok et al. 1998; Sahai et al. 1998). We note that the typical time separation of these arcs in AGB stars and protoplanetary nebulae is a few hundred years (Kwok et al. 2001), which is comparable to the estimates of the dynamical ages of the cones.

If we examine the images of Figures 2 and 3 closely, it is also possible that there is another smaller pair of cones, represented by fainter fans with sides defined by a pair of straight lines oriented at P.A. 324° and 356°, suggesting that the symmetry axis lies at a PA of −20°. The cones, with a common axis oriented at an angle of 20° ± 5° from the plane of the sky, have an opening angle of 0.077 ± 0.03π, and radii of 222 ± 8 and 270 ± 8 arcsec, respectively. A sketch of the multipolar structure is given in Figure 7. Multipolar structures have been seen in the planetary nebulae NGC 2440 (López et al. 1998) and NGC 6309 (Vázquez et al. 2008), and in other young planetary nebulae (Sahai 2000), and it is possible that NGC 6853 also belongs to this class. The similarity in size of the two pairs of bipolar cones suggests that they have similar dynamical ages, or that they were formed within a relatively short ($\sim 10^2$ yr) time span. In this regard, NGC 6853 is similar to NGC 2440 and NGC 6309.

The side boundaries of the two cones are relatively well defined in the H_2 image, suggesting that the outflows are confined by an external medium of neutral material. The outer edges, in particular the northern one, indicate the area of interaction with the remnant AGB wind. The filamentary appearance of the outer edge may represent the breakout of the fast flow. This can be identified in the "flowery petals" seen in NGC 6720 (Fig. 6). The radial rays emanating from a torus are probably counterparts of the bipolar radial rays in NGC 6853, as shown in Figures 2 and 4.

The sharp cone boundaries do require that the fast outflows are extremely well collimated. Alternatively, the boundaries of the cones may be due to angular sweeping of a precessing jet. If this is the case, then the interaction between the fast outflow and the AGB wind is limited to the rims of the cones, and the radial rays are projections of the jet at different orientations. Evidence for precessing outflows already exists for a number of planetary nebulae (NGC 6884, Miranda et al. 1999; IRAS 17441−2411, Volk et al. 2007; NGC 6309, Vázquez et al. 2008). The agent driving the precessing jet needs to be very compact, probably an accretion disk around a central binary system.

4. CONCLUSIONS

If two of the best-observed planetary nebulae have the same intrinsic structure, is this model universal for all planetary nebulae? This hypothesis is difficult to test, as most planetary nebulae are distant and have not been observed to the same degree of sensitivity, dynamical range, and spatial resolution. Another nearby nebula, NGC 7293 (the Helix Nebula), also shows radial rays and well-defined outer halos (Hora et al. 2006) and multipolar structures (O'Dell et al. 2004). What is clear, however, is that morphology classifications based on the apparent shape of the main, bright parts of the nebula is not a good indicator of the nebula's intrinsic structure. These observations have shown us that even after over 200 years of study, our knowledge on the basic morphology of planetary nebulae is still primitive. Observations with a variety of techniques are needed to reveal the rich structure of planetary nebulae and to understand their dynamical origins.

This work is based on observations obtained at the Canada-France-Hawaii Telescope (CFHT) which is operated by the National Research Council of Canada, the Institut National des Sciences de l'Univers of the Centre National de la Recherche Scientifique of France, and the University of Hawaii. Access to the CFHT was made possible by the Ministry of Education and the National Science Council of Taiwan as part of the Cosmology and Particle Astrophysics (CosPA) initiative. The work was supported by a grant from the Research Grants Council of the Hong Kong Special Administrative Region, China (project HKU 7028/07P).

REFERENCES

Balick, B. 1987, AJ, 94, 671

Balick, B., Gonzalez, G., Frank, A., & Jacoby, G. 1992, ApJ, 392, 582

Benedict, G. F., et al. 2003, AJ, 126, 2549

Bryce, M., Balick, B., & Meaburn, J. 1994, MNRAS, 266, 721

Goad, L. E. 1975, Ph.D. Thesis, The Structure of Planetary Nebulae, Harvard University

Guerrero, M. A., Manchado, A., & Chu, Y.-H. 1997, ApJ, 487, 328

Hora, J. L. 2006, IAU Symp. 234, Planetary Nebulae in our Galaxy and Beyond, ed. M. J. Barlow & R. H. Mendez (Cambridge: Cambridge Univ. Press), 173

Hora, J. L., Latter, W. B., Smith, H. A., & Marengo, M. 2006, ApJ, 652, 426

Hua, C. T., Dopita, M. A., & Martinis, J. 1998, A&AS, 133, 361

Hua, C. T., & Louise, R. 1970, A&A, 9, 448

Kastner, J. H., Weintraub, D. A., Gatley, I., Merrill, K. M., & Probst, R. G. 1996, ApJ, 462, 777

Kupferman, P. N. 1983, ApJ, 266, 689

Kwok, S. 2000, Origin and Evolution of Planetary Nebulae (Cambridge: Cambridge Univ. Press)

Kwok, S., Su, K. Y. L., & Hrivnak, B. J. 1998, ApJ, 501, L117

Kwok, S., Su, K. Y. L., & Stoesz, J. A. 2001, in Post-AGB Objects as a Phase of Stellar Evolution, R. Szczerba & S. K. Gorny (Dordrecht: Kluwer), 115

López, J. A., Meaburn, J., Bryce, M., & Holloway, A. J. 1998, ApJ, 493, 803

Mauron, N., & Huggins, P. J. 1999, A&A, 349, 203

Meaburn, J., Boumis, P., Christopoulou, P. E., Goudis, C. D., Bryce, M., & Lopez, J. A. 2005, Rev. Mex. AA, 41, 109

Minkowski, R., & Osterbrock, D. 1960, ApJ, 131, 537

Miranda, L. F., Guerrero, M. A., & Torrelles, J. M. 1999, AJ, 117, 1421

O'Dell, C. R., McCullough, P. R., & Meixner, M. 2004, AJ, 128, 2339

Proisy, P. E. 1974, A&A, 35, 71

Sahai, R. 2000, ApJ, 537, L43

Sahai, R., et al. 1998, ApJ, 493, 301

Vázquez, R., et al. 2008, A&A, 481, 107

Volk, K., Kwok, S., & Hrivnak, B. J. 2007, ApJ, 670, 1137

Zuckerman, B., & Gatley, I. 1988, ApJ, 324, 501